optica

Single-branch Er:fiber frequency comb for precision optical metrology with 10^{-18} fractional instability

HOLLY LEOPARDI,[1,2,*] JOSUE DAVILA-RODRIGUEZ,[2] FRANKLYN QUINLAN,[2] JUDITH OLSON,[1,2] JEFF A. SHERMAN,[2] SCOTT A. DIDDAMS,[1,2] AND TARA M. FORTIER[1,2,3]

[1]*Department of Physics, University of Colorado Boulder, 440 UCB Boulder, Colorado 80309, USA*
[2]*Time and Frequency Division, National Institute of Standards and Technology, Boulder, Colorado 80305, USA*
[3]*e-mail: tara.fortier@nist.gov*
Corresponding author: holly.leopardi@colorado.edu

The comparison of optical atomic clocks with frequency instabilities reaching 1 part in 10^{16} at 1 s will enable more stringent tests of fundamental physics. These comparisons, mediated by optical frequency combs, require optical synthesis and measurement with a performance better than, or comparable to, the best optical clocks. Fiber-based mode-locked lasers have shown great potential for compact, robust, and efficient optical clockwork but typically require multiple amplifier and fiber optic paths that limit the achievable fractional frequency stability near 1 part in 10^{16} at 1 s. Here we describe an erbium-fiber laser frequency comb that overcomes these conventional challenges by ensuring that all critical fiber paths are common mode and within the servo-controlled feedback loop. Using this architecture, we demonstrate a fractional optical measurement uncertainty below 1×10^{-19} and fractional frequency instabilities less than 3×10^{-18} at 1 s and 1×10^{-19} at 1000 s.   © 2017 Optical Society of America

OCIS codes: (120.3940) Metrology; (320.7090) Ultrafast lasers; (140.4050) Mode-locked lasers; (120.4800) Optical standards and testing.

https://doi.org/10.1364/OPTICA.4.000879

1. INTRODUCTION

Optical atomic clocks, which provide both stable and accurate timing with up to 18 digits of resolution [1–4], represent extremely sensitive tools with which to study fundamental physics. For instance, fine changes in the relative frequency of optical atomic clock transitions can be used to detect possible time variations of fundamental constants [5–9], changes in gravitational potentials at the centimeter scale [10], and could potentially be used for dark matter and gravitational wave detection [11,12]. However, these measurements often require the comparison of clocks based on different atomic species, whose transition frequencies can be separated by hundreds of terahertz. Optical frequency combs (OFCs) provide a means to bridge the gap in frequency between optical atomic clocks, allowing for the relative comparison of optical atomic clock transitions as well as absolute comparison to the current microwave atomic reference in ^{133}Cs [13–15]. While OFCs have been an enabling technology in optical clock development, their ability to synthesize optical and microwave frequencies from atomic frequency standards and references has led to a host of additional applications [16], including atmospheric trace gas detection [17,18], calibration of astronomical spectrographs [19,20], ultra-low-noise microwave generation [21,22], optical time and frequency transfer [23–28], as well as synchronization in large-scale science facilities [29–31].

In the past decade, there have been significant improvements in the performance of optical reference cavities that serve as the local oscillator in optical atomic clocks. The development of high mechanical quality factor mirror coatings [32] and the operation of optical reference cavities at cryogenic temperatures [33,34] are projected to increase the stability of atomic clocks by nearly an order of magnitude over the current state of the art. Consequently, high-fidelity frequency synthesis with these optical frequency references will require optical frequency comb sources with equally good or better performance.

Er:fiber-based optical frequency combs are widely used as optical synthesizers and dividers because they facilitate the possibility of compact design as well as robust and turnkey operations [35–37]. These advantages are in contrast to traditional Ti:sapphire-based OFCs, which have been the "gold standard" in terms of performance [38–40], but do not offer the immediate possibility for robust or continuous long-term operation. One drawback of Er:fiber-based OFCs is their natively low average output power (<100 mW) and repetition rate (<250 MHz), which often requires them to employ separate amplifiers and nonlinear fibers to access multiple optical frequency references [41,42]. This is often required because it is difficult to optimize the broadened spectrum generated in highly nonlinear fiber (HNLF) for simultaneous detection of multiple optical beat signals. Although more convenient for signal optimization, this
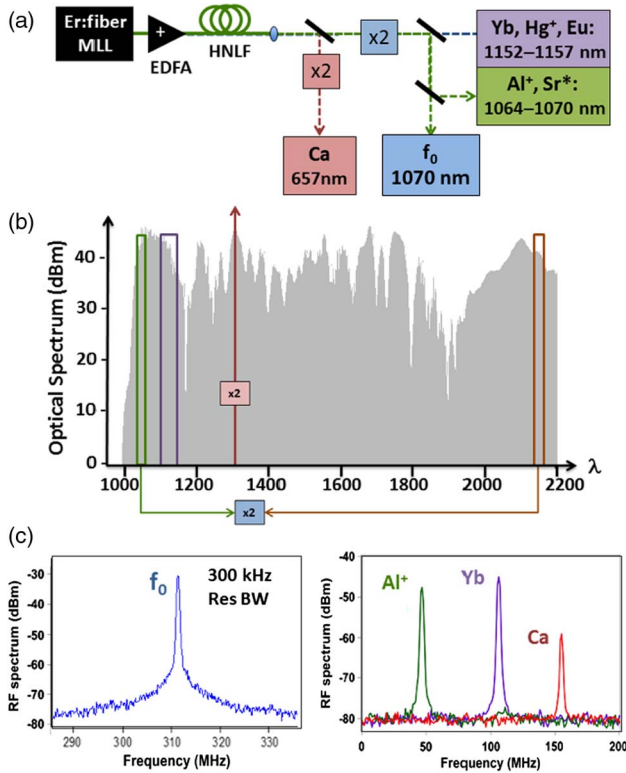
Fig. 1. (a) Block diagram highlighting the single-branch OFC architecture. (b) The optical spectrum after optical amplification and external broadening in PM highly nonlinear fiber and its overlap with the various optical frequency standards and references at the National Institute of Standards and Technology (NIST), Boulder. Colors correspond to wavelength regions highlighted in (a). (c) The optical offset frequency detected near 1070 nm in a 300 kHz resolution bandwidth. Optical heterodyne beat signals shown in a 300 kHz resolution bandwidth between the optical spectrum in Fig. 1(b) with the Al^+ clock laser at 1070 nm in green, the ytterbium lattice clock laser at 1157 nm in purple, and the Ca clock laser at 657 nm in red. These signals are offset from each other by arbitrary frequencies to show the relative strengths of the signal.

"multibranch" configuration results in uncompensated fiber paths that are outside the feedback loop of the laser and hence limit the measurement stability of these OFCs near or above one part in 10^{16} at 1 s averaging [41,43]. This level of residual noise is barely sufficient to support the current state of the art in optical atomic clocks [1,2,4,44] and is significantly higher than the level required to support the reported stability of cryogenic optical cavities [33,34]. Here we demonstrate an alternative "single-branch" detection scheme [45,46] for optical comparisons [see Fig. 1(a)] that enables direct measurement of optical frequencies with millihertz resolution. Our approach uses a single optical amplifier and nonlinear fiber that are within the laser feedback loop and common to all optical paths. By designing the measurement architecture to be maximally common mode, we minimize the additive measurement instabilities and enable the comparison of optical atomic frequency references with a 1 mHz frequency resolution in 1 s of averaging.

2. FREQUENCY COMPARISONS USING AN OFC

The optical spectrum from a mode-locked laser that is used in optical comparisons is often referred to as a frequency comb since

its spectrum, comprised of hundreds of thousands of equally spaced optical modes, resembles a fine-toothed comb in the frequency domain. A special characteristic of the frequency comb is that passive mode-locking of the longitudinal laser modes during pulse formation imposes a simple frequency relationship between the optical modes in the spectrum. As such, all optical modes in the spectrum can be related by two radio frequencies (RFs): the laser repetition rate, f_{rep}, which determines the mode spacing and an overall offset from 0 Hz, f_0. Using these two characteristic frequencies, any arbitrary optical mode at ν_N (with harmonic order N typically $\sim 1,000,000$ in a fiber-based system) of the comb can be defined as

$$\nu_N = N \times f_{rep} + f_0. \tag{1}$$

With the values of f_0 and f_{rep} either measured against or defined by the ^{133}Cs primary reference, the optical comb can then be used as an absolute reference against which to compare and measure an unknown optical frequency. More specifically, the measurement of an optical frequency, ν_{opt1}, is performed by measuring the RF heterodyne beat signal, fb_{opt1}, between the single tooth of the comb, N, and the reference clock laser. The mode number, N, is calculated using knowledge of f_{rep} and by measuring ν_{opt1} using a wavemeter. Thus, the optical frequency is defined as

$$\nu_{opt1} = N \times f_{rep} + f_0 + fb_{opt1}. \tag{2}$$

From Eq. (2), we see that the comb provides a means for optical-to-microwave conversion and vice versa. In the measurements presented here, we stabilize the modes of the OFC to an optical reference. This is achieved by tight phase-locking of the beat signals fb_{opt1} and f_0 to hydrogen-maser referenced frequencies. This technique fixes the frequency comb at two points: one at mode N near ν_{opt1}, and the second in the RF domain at f_0. Stabilization of the OFC in this manner transfers the phase and frequency information of the optical reference to f_{rep} and hence to every mode in the OFC. Measurement of the heterodyne beat signal of a second optical reference, fb_{opt2}, against mode number M then provides a frequency comparison of the two optical references via the optical comb as follows:

$$\nu_{opt2} = \frac{M}{N}(\nu_{opt1} - f_0 - fb_{opt1}) + f_0 + fb_{opt2}. \tag{3}$$

From Eq. (3), we see that one optical reference can be defined as a small correction to the ratio of the comb modes, $\frac{M}{N}$. While Eq. (3) describes an optical frequency comparison using an OFC, we are interested in determining the instability added by the OFC to the measurement of the references ν_{opt1} and ν_{opt2}. In the following sections, we describe the Er:fiber laser and the single-branch measurement architecture we use for optical comparisons as well as the measurement technique used to evaluate the total measurement noise.

A. Single-Branch Er:Fiber-Based OFC

The OFC in our measurements is based on a self-referenced 180 MHz repetition rate Er:fiber ring laser whose 1550 nm pulse train is generated via nonlinear polarization evolution [47]. The laser operates with an average output power of 90 mW and an optical bandwidth of $\sim$80 nm FWHM directly from the laser cavity. In our experimental setup, the output of the laser is amplified in a polarization maintaining (PM) erbium-doped fiber optical amplifier (EDFA). Pumped with two 980 nm laser diodes at approximately 700 mW each, the optical pulses at the output

of the EDFA have an autocorrelation width of <70 fs and an average power of 270 mW. Light from the EDFA is then directly fiber-coupled to 40 cm of PM-HNLF [48] with a total throughput of >80%. The HNLF enables broadening from 980 nm to 2200 nm and allows for simultaneous beat-note detection of f_0 as well as access to the transfer oscillators for the following optical references [see Fig. 1(b)]: the Ca atomic beam clock at 657 nm (from doubled comb light at 1314 nm), the Eu^{3+}:Y_2SiO_5 spectral hole optical reference (1157 nm/2), as well as transfer lasers from the following optical atomic clocks: the Yb optical lattice clock (1157 nm/2), the Al^+-ion clock (1070 nm/4), the Hg^+-ion clock (1126 nm/4), and the Sr optical lattice clock (1064 nm transfer oscillator sent from JILA to NIST via an optical frequency comb at JILA). Due to the relatively long length of HNLF, we still observe significant structure on the broadened output spectrum. However, the use of only PM fiber components outside the laser enables stability of the power and spectral shape output from the HNLF.

For stabilization of the OFC, and for the measurement and comparison of the different optical atomic clock lasers, the output spectrum from the PM-HNLF is split into four separate free-space optical interferometers to obtain a heterodyne beat signal against the different clock lasers. Figure 1(c) shows one beat signal from each of the four spectral regions, which can access optical signals over a range of several tens of nanometers with similar power per mode. Aside from the optical beat signal at 657 nm, the other heterodyne signals are obtained with at least 30 dB SNR when measured with a 300 kHz resolution bandwidth, which allows for direct locking and counting of the optical beat signals without the need for tracking oscillators.

In order to minimize the timing errors contributed by the optical interferometer paths, the entire OFC setup is enclosed in a 1" thick acrylic box. The maximum noncommon mode optical interferometer paths were less than 1 m. Separate PPLN crystals are used for doubling light at 1314 nm to access the Ca clock laser at 657 nm and for doubling 2140 nm for self-referenced detection of f_0. Dividing the spectrum at the output of the HNLF with dichroic beam splitters and reusing light from the $f - 2f$ interferometer allows for efficient use of the broadened spectrum.

As mentioned above, knowledge of f_0 is critical for characterization of optical frequencies. The simplest detection of f_0 uses a self-referencing technique that compares frequencies, N and $2N$, separated by an optical octave via frequency doubling of mode N, whereby

$$2 \times \nu_N - \nu_{2N} = f_0. \tag{4}$$

To measure f_0, the optical beat signal between doubled light at the low-frequency end of the spectrum (~2140 nm) is compared against that at the high-frequency end of the spectrum at ~1070 nm using the f_0 interferometer as depicted in Fig. 1(a). Photodetection of the optical f_0 beat results in an RF signal that is filtered, amplified, and compared against a hydrogen-maser referenced synthesizer. The resulting error signal is used in a feedback loop that actuates on a single OFC pump laser at 980 nm with approximately 150 kHz of bandwidth. Similarly, the laser repetition rate is stabilized by photodetecting the optical heterodyne beat signal between one mode of the OFC and one of the optical frequency references. The resulting RF signal is filtered, amplified, and compared against a second hydrogen-maser referenced synthesizer. The resulting error signal is sent to an

intracavity EOM for fast control (~300 kHz bandwidth) of the laser cavity length and to a piezoelectric transducer to compensate for long-range cavity drift.

3. MEASUREMENT INSTABILITY AND DISCUSSION

For measurement of the optical instability added by the frequency comb when comparing optical references, we utilize a simple and powerful approach depicted in Fig. 2(a). This technique employs
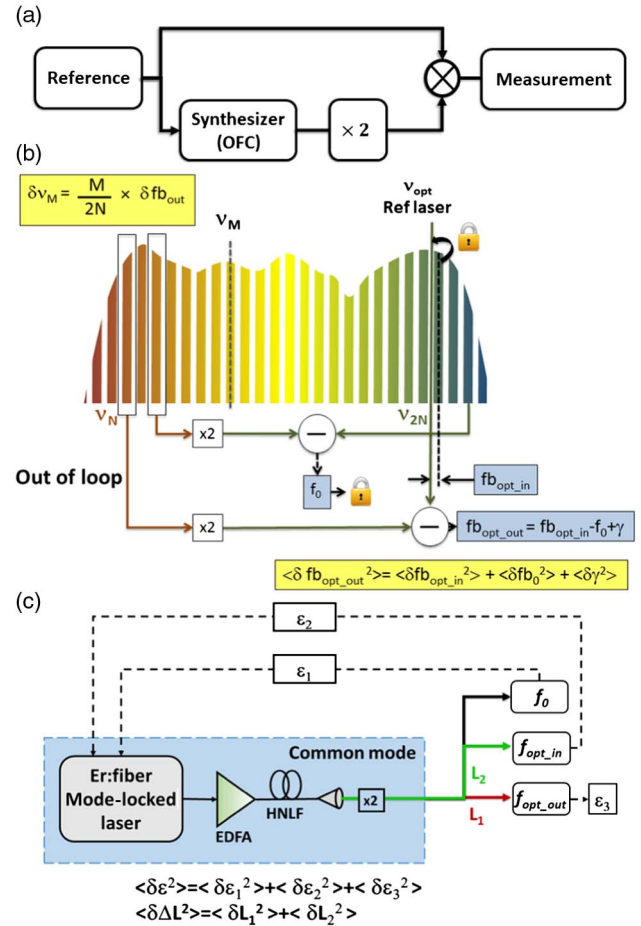
Fig. 2. (a) Simplified diagram of the single-comb measurement technique. The OFC is referenced to a cw laser, and a synthesized frequency an octave away is then doubled to that of the incoming light. This doubled light is then mixed with the original cw laser to determine the performance of the device under test, namely, the OFC and PPLN crystal used for doubling. (b) The single-comb measurement technique used to characterize the instability added by the single-branch OFC to an out-of-loop optical frequency measurement. Here fb_{opt_in} measures the in-loop optical beat signal between the reference laser and the frequency comb that is used for stabilization of the laser repetition rate. To determine the instability the OFC adds across an octave, the long wavelength end of the spectrum is doubled and heterodyned against the same reference laser used to stabilize the repetition rate. This optical beat signal, fb_{opt_out}, measures the out-of-loop contributions of the offset frequency, f_0, and the locked beat, fb_{opt_in}, since there are optical and electronic paths that are not common to the measurement of fb_{opt_out}. (c) Block diagram highlighting the individual noise contributions within the optical frequency comb setup to measurement of an optical frequency reference at 282 THz. The instability contributed by out-of-loop electronics is labeled with ε and noncommon path lengths with L.

an optical reference laser whose output is split into two paths. In the lower path, the reference laser controls the OFC, which synthesizes frequencies at harmonics of the repetition rate. The low-frequency components synthesized by the OFC are then frequency doubled and compared against the original reference laser. Essentially, this approach amounts to a combined test of the OFC and frequency doubling via second-harmonic generation, which have both been established as a valid techniques in earlier experiments [38,49,50]. We further note that variations of the interferometric approach as depicted in Fig. 2(a) are common in all of the frequency metrology for evaluating oscillators, synthesizers, and frequency multipliers and dividers [51]. This approach to evaluating the instability of the OFC has the advantage of simplicity in not requiring a second frequency comb and the additional optical interferometer needed for its heterodyne comparison.

As mentioned previously, to ensure coherent optical synthesis, both the offset frequency, f_0, and the repetition rate, f_{rep} are tightly phase-locked. Specifically, f_{rep} is stabilized by locking the heterodyne beat, fb_{opt_in}, between mode $2N$ of the comb and the optical reference at 1064 nm [Fig. 2(b)], such that

$$\nu_{opt} = 2N \times f_{rep} + f_0 + fb_{opt\_in}. \tag{5}$$

The OFC under test transfers the frequency information of the optical reference near mode ν_{2N} to the frequency ν_N, which is an octave away at half the reference frequency. During this synthesis step, the OFC will contribute some excess frequency error, γ, which we are interested in quantifying. We quantify this error by frequency doubling ν_N using second-harmonic generation in a nonlinear crystal, back to the initial reference frequency near ν_{2N}. This frequency-doubled light, synthesized by the OFC, is then compared against the original optical reference, ν_{opt}. In this comparison, we measure

$$\nu_{opt} - 2(N \times f_{rep} + f_0) + \gamma = fb_{opt\_out}. \tag{6}$$

By combining Eqs. [5] and [6], we find that

$$fb_{opt\_out} = fb_{opt\_in} - f_0 + \gamma. \tag{7}$$

Hence, in this comparison, we isolate the frequency error γ from the in-loop residual instabilities fb_{opt_in} and f_0. Not captured in Eq. [7] is the instability contributed by frequency doubling, which has been demonstrated to perform at the 10^{-19} level, largely limited by technical noise, while calculations predict that the fundamental limit to frequency doubling should be at the 10^{-21} level [52,53]. Thus, the excess instability, $\langle \delta \gamma^2 \rangle$, is mainly due to the OFC and any noncommon electronic and optical paths within the feedback loops.

A similar evaluation can be performed using a second OFC, where instead of frequency doubling the ν_N mode to $2 \times \nu_N$ and comparing against the same optical reference, a second OFC is also locked to the original reference, and the two combs are heterodyned directly [39,45] or with an intermediate cw laser [46]. In Fig. 2(a), for this technique there would be a second synthesizer in the top branch and doubling would not be required, as any frequencies of the two OFC synthesizers can be directly compared. This measurement, while allowing flexibility in which frequencies are measured, will contain excess instability of similar order to the OFC under test. To ascertain the limit on a single OFC, one would then have to assume that the measured noise is the combined noise of two similar but uncorrelated OFCs.

Additionally, this measurement will contain a noise contribution from the optical interferometer needed for the heterodyne comparison between the two combs. Our measurement avoids these ambiguities.

In general, complete characterization of the measurement noise in an optical frequency comparison must also account for additional noise terms unique to the interferometers used to measure the second optical reference. Therefore, the signal-to-noise ratio of the heterodyne beats with various optical references and measurements of the contribution of the noncommon electrical and optical paths must be performed. Combined, these measurements then allow us to determine the total instability contributed in optical synthesis using a single OFC.

In the single-branch architecture for our Er:fiber-based OFC, all optical fiber components are within the feedback loops of the laser and are common to all optical paths. Consequently, stabilization of f_0 and fb_{opt_in} compensates for the noise of these optical components for all optical interferometers. However, there is additive noise of optical and electronic components within the feedback loops that are *not* common to the measurement of a second or third optical standard. Additionally, the noise contributed by components unique to the measurement of other optical references will adversely affect their measured stability. Figure 2(c) is a block diagram representation of how we visualize the different optical and electronic instability contributions from the OFC setup.

Isolating and measuring the individual noise contributions from the measurement architecture allows us to determine the noise inherent in performing an optical comparison at any frequency across the comb. Figure 3 shows the total and itemized measurement instabilities. Full details of the individual measurements, as well as details pertaining to the frequency counting, can be found in Supplement 1. Briefly, the instabilities of all the RF beat signals were measured using an Agilent 53132A frequency counter (this is not an endorsement by the U.S. government). While these counters are accurate for measuring Allan deviations
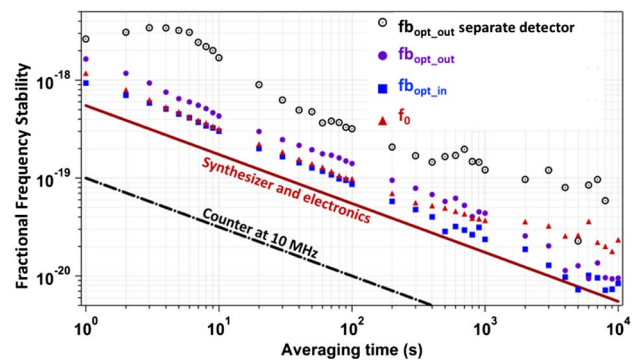
Fig. 3. Itemized residual noise contributions of the single-branch OFC to an optical measurement at 282 THz measured with a 0.5 Hz noise-equivalent bandwidth. The red triangles and blue squares measure the residual noise in the f_0 and fb_{opt_in} phase-locked loops, respectively. The residual noise across the octave of an out-of-loop beat, fb_{opt_out}, measured on the same detector (purple circles) and separate detector (black circles) as fb_{opt_in}. The black circles show the upper limit to the noise added by two 50 cm free-space interferometers. The total contributions from the amplifier chains and the synthesizers are shown as the red solid line. The contribution of the measurement instability in counting a 10 MHz signal is shown in black. It is important to note that the counterinstability will scale linearly with the measured frequency.

for signals dominated by white frequency noise, there is concern about the accuracy in their measurement of signals dominated by white phase noise [54]. A discussion of this can be found in Supplement 1, detailing a measurement whereby we ascertained the instability of a single RF beat signal by using three alternative methods.

To determine the contribution of a free-space interferometer, we measured fb_{opt_out} on the same detector as fb_{opt_in} (purple circles in Fig. 3) and on a separate detector (black circles in Fig. 3). From our measurements, we determined that the instability added by the OFC to the measurement of a second or third out-of-loop optical measurement at 282 THz is 2.6×10^{-18} at 1 s. This instability is largely limited by the combined 100 cm of differential free-space path lengths from the in- and out-of-loop optical interferometers. These contribute instabilities at the level shown by the black empty circles in Fig. 3. Air path fluctuations and differential optical paths for the two ends of the OFC spectrum in both fiber and free-space components are most likely responsible for the excess instability, such that the total instability of our system can be further reduced by shortening the uncompensated free-space optical interferometer paths, purging the acrylic enclosure, or by measuring multiple optical heterodynes on the same detector.

While we have been careful to characterize instabilities contributed by the OFC by comparing extreme ends of the spectrum and individually characterizing noise added by noncommon components, there may be additional optical frequency-dependent noise contributed by the broadening process in the EDFA HNLF system. For example, ASE from the EDFA seeded into the HNLF could result in an increased white phase noise floor. This broadband noise would manifest itself as a reduction in the signal-to-noise ratio of the heterodyne signal of the optical comparison. Supplement 1 details a measurement performed, whereby we verified that changes in the SNR from 25 dB to 40 dB of the in- and out-of-loop beat signals resulted in changes in the 1 s instability at a level below 7×10^{-19}.

An assumption, and potential limitation, of our measurement is that the fractional instability is deterministic across the comb, as governed by $\nu_N = N \times f_{rep} + f_0$. Remarkably, our measurements, as well as those of many others in the community, have continued to verify the validity of this simple and powerful expression. Nonetheless, it is worth considering possible sources that might lead to deviations as still higher levels of precision are explored. There will likely always be challenging technical limits, such as uncorrelated wavelength-dependent noise that arises from small out-of-loop paths. These could be reduced with still better mechanical stability and active path stabilization. However, it is interesting to consider more fundamental noise sources, such as intensity noise on the pulse train that may be converted to phase noise on the comb in the HNLF [55]. In principle, shot noise on the input pulse train could lead to nonuniform wavelength-dependent noise through the nonlinear propagation and amplification in the HNLF. While not observed previously, determining the limitation imposed by this amplitude to phase conversion could be addressed through a combination of modeling and measurements at multiple wavelengths across the octave bandwidth of the comb. Such experiments would be an interesting topic of further study.

In addition to the stability, accuracy is also necessary when comparing frequency references. We can place an upper limit
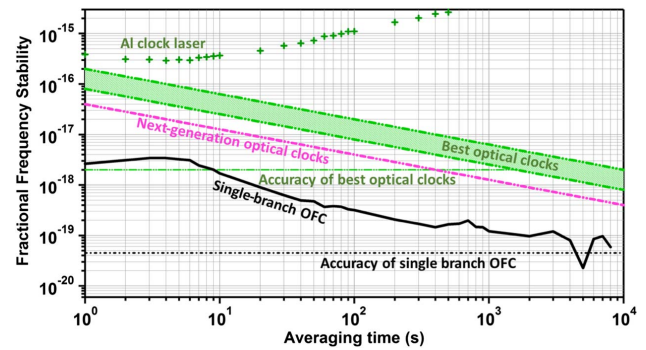
Fig. 4. Residual instability and accuracy of the single-branch Er:fiber OFC (solid black lines), as well as the instability and accuracy of state-of-the-art optical cavities and optical atomic clocks (green dashed lines) [1–4]. The pink dashed line represents the theoretical next-generation optical atomic clocks based on a cryogenic optical cavity [33,34]. Additionally, we show the optical comparison between a Yb lattice clock laser and an Al+-ion clock laser with the single-branch OFC (green crosses).

on the frequency offsets contributed by the single-branch OFC at $1.3 \times 10^{-20} \pm 4.5 \times 10^{-20}$ on a 282 THz carrier. This offset was determined by comparing the average value of fb_{opt_out} to that of the expected maser referenced value using a frequency time record with greater than 10,000 seconds of data (from the data of Fig. 3). Additional data acquired over 100,000 seconds shows further reduction in the frequency offset of the single-branch comb to $1.4 \times 10^{-21} \pm 1.7 \times 10^{-20}$ on a 282 THz carrier. Since Er:fiber-based OFCs have been demonstrated to contribute even smaller offsets [56], we expect that this upper bound is currently limited simply by the measurement time. However, to achieve still lower uncertainties, temperature-dependent frequency shifts of the RF synthesizers and components may need to be characterized and stabilized. Alternatively, synthesizing the RF reference frequencies with the OFC itself [57,58] should reduce the total measurement error.

Finally, to demonstrate that the single-branch OFC can support the current best optical frequency references at NIST, we performed an optical comparison between the Yb lattice clock laser at 1157 nm and the Al+ quantum logic clock laser at 1070 nm. Approximately 3 mW of optical power from each optical standard was transferred via actively noise-canceled fibers [59] across approximately 30 m of fiber. As seen in Fig. 4, the optical comparison yielded a 1 s fractional frequency instability of 3.84×10^{-16} limited by the Al-clock laser. This level is almost two orders of magnitude higher in instability than the excess noise added by the single-branch OFC, showcasing the contrast in performance between the single-branch OFC and current optical atomic clock lasers.

4. CONCLUSIONS

In summary, we have developed and characterized the performance of an Er:fiber frequency comb using a single-branch measurement architecture for the synthesis and comparison of optical atomic clocks. In our single-branch configuration, the Er:fiber comb utilized a single PM-EDFA and PM-HNLF that were both within the laser feedback loop and common to all optical interferometers for stabilization of the offset frequency as well as for

characterization of the six optical standards at NIST. We found that the total synthesis and measurement instability contributed by the OFC was less than 3×10^{-18} at 1 s and 1×10^{-19} at 1000 seconds on a 282 THz optical carrier. Additionally, the frequency offsets contributed by the OFC to an out-of-loop measurement are $1.4 \times 10^{-21} \pm 1.7 \times 10^{-20}$ on a 282 THz carrier. As summarized in Fig. 4, this instability is nearly two orders of magnitude below the reported 1 s instability of the current state of the art in optical atomic clocks [1,2,4] and is one order of magnitude lower than the projected stability for next-generation optical atomic clocks using a clock laser stabilized to a cryogenic optical cavity [33].

Finally, these measurements demonstrate that a single-branch Er:fiber comb can perform at a similar level to OFCs based on Ti:sapphire lasers [38,40]. As a result, a single-branch OFC based on an Er:fiber laser can support both the state-of-the-art optical frequency references of today as well as those of the future.

See Supplement 1 for supporting content.

REFERENCES

1. B. J. Bloom, T. L. Nicholson, J. R. Williams, S. L. Campbell, M. Bishof, X. Zhang, W. Zhang, S. L. Bromley, and J. Ye, "An optical lattice clock with accuracy and stability at the 10^{-18} level," Nature **506**, 71–75 (2014).
2. N. Hinkley, J. A. Sherman, N. B. Phillips, M. Schioppo, N. D. Lemke, K. Beloy, M. Pizzocaro, C. W. Oates, and A. D. Ludlow, "An atomic clock with 10^{-18} instability," Science **341**, 1215–1218 (2013).
3. M. Schioppo, R. Brown, W. McGrew, N. Hinkley, R. Fasano, K. Beloy, T. Yoon, G. Milani, D. Nicolodi, and J. Sherman, "Ultrastable optical clock with two cold-atom ensembles," Nat. Photonics **11**, 48–52 (2017).
4. T. Nicholson, S. Campbell, R. Hutson, G. Marti, B. Bloom, R. McNally, W. Zhang, M. Barrett, M. Safronova, and G. Strouse, "Systematic evaluation of an atomic clock at 2×10^{-18} total uncertainty," Nat. Commun. **6**, 6896 (2015).
5. T. M. Fortier, N. Ashby, J. C. Bergquist, M. J. Delaney, S. A. Diddams, T. P. Heavner, L. Hollberg, W. M. Itano, S. R. Jefferts, K. Kim, F. Levi, L. Lorini, W. H. Oskay, T. E. Parker, and J. E. Stalnaker, "Precision atomic spectroscopy for improved limits on variation of the fine structure constant and local position invariance," Phys. Rev. Lett. **98**, 070801 (2007).
6. T. Rosenband, D. B. Hume, P. O. Schmidt, C. W. Chou, A. Brusch, L. Lorini, W. H. Oskay, R. E. Drullinger, T. M. Fortier, J. E. Stalnaker, S. A. Diddams, W. C. Swann, N. R. Newbury, W. M. Itano, D. J. Wineland, and J. C. Bergquist, "Frequency ratio of Al+ and Hg+ single-ion optical clocks; metrology at the 17th decimal place," Science **319**, 1808–1812 (2008).
7. N. Huntemann, B. Lipphardt, C. Tamm, V. Gerginov, S. Weyers, and E. Peik, "Improved limit on a temporal variation of m_p/m_e from comparisons of Yb+ and Cs atomic clocks," Phys. Rev. Lett. **113**, 210802 (2014).
8. M. Fischer, N. Kolachevsky, M. Zimmermann, R. Holzwarth, T. Udem, T. W. Hansch, M. Abgrall, J. Grunert, I. Maksimovic, S. Bize, H. Marion, F. P. Dos Santos, P. Lemonde, G. Santarelli, P. Laurent, A. Clairon, C. Salomon, M. Haas, U. D. Jentschura, and C. H. Keitel, "New limits on the drift of fundamental constants from laboratory measurements," Phys. Rev. Lett. **92**, 230802 (2004).
9. R. M. Godun, P. B. R. Nisbet-Jones, J. M. Jones, S. A. King, L. A. M. Johnson, H. S. Margolis, K. Szymaniec, S. N. Lea, K. Bongs, and P. Gill, "Frequency ratio of two optical clock transitions in Yb-171(+) and constraints on the time variation of fundamental constants," Phys. Rev. Lett. **113**, 210801 (2014).
10. C. W. Chou, D. B. Hume, T. Rosenband, and D. J. Wineland, "Optical clocks and relativity," Science **329**, 1630–1633 (2010).
11. S. Kolkowitz, I. Pikovski, N. Langellier, M. D. Lukin, R. L. Walsworth, and J. Ye, "Gravitational wave detection with optical lattice atomic clocks," Phys. Rev. D **94**, 124043 (2016).
12. A. Derevianko and M. Pospelov, "Hunting for topological dark matter with atomic clocks," Nat. Phys. **10**, 933–936 (2014).
13. T. Rosenband, P. O. Schmidt, D. B. Hume, W. M. Itano, T. M. Fortier, J. E. Stalnaker, K. Kim, S. A. Diddams, J. C. J. Koelemeij, J. C. Bergquist, and D. J. Wineland, "Observation of the S-1(0)->(3)P0 clock transition in Al-27(+)," Phys. Rev. Lett. **98**, 220801 (2007).
14. M. Takamoto, F.-L. Hong, R. Higashi, and H. Katori, "An optical lattice clock," Nature **435**, 321–324 (2005).
15. H. S. Margolis, G. P. Barwood, G. Huang, H. A. Klein, S. N. Lea, K. Szymaniec, and P. Gill, "Hertz-level measurement of the optical clock frequency in a single 88Sr+ ion," Science **306**, 1355–1358 (2004).
16. S. A. Diddams, "The evolving optical frequency comb," J. Opt. Soc. Am. B **27**, B51–B62 (2010).
17. F. Adler, P. Masłowski, A. Foltynowicz, K. C. Cossel, T. C. Briles, I. Hartl, and J. Ye, "Mid-infrared Fourier transform spectroscopy with a broadband frequency comb," Opt. Express **18**, 21861–21872 (2010).
18. M. J. Thorpe, K. D. Moll, R. J. Jones, B. Safdi, and J. Ye, "Broadband cavity ringdown spectroscopy for sensitive and rapid molecular detection," Science **311**, 1595–1599 (2006).
19. T. Steinmetz, T. Wilken, C. Araujo-Hauck, R. Holzwarth, T. W. Hansch, L. Pasquini, A. Manescau, S. D'Odorico, M. T. Murphy, T. Kentischer, W. Schmidt, and T. Udem, "Laser frequency combs for astronomical observations," Science **321**, 1335–1337 (2008).
20. G. G. Ycas, F. Quinlan, S. A. Diddams, S. Osterman, S. Mahadevan, S. Redman, R. Terrien, L. Ramsey, C. F. Bender, B. Botzer, and S. Sigurdsson, "Demonstration of on-sky calibration of astronomical spectra using a 25 GHz near-IR laser frequency comb," Opt. Express **20**, 6631–6643 (2012).
21. T. M. Fortier, M. S. Kirchner, F. Quinlan, J. Taylor, J. C. Bergquist, T. Rosenband, N. Lemke, A. Ludlow, Y. Jiang, C. W. Oates, and S. A. Diddams, "Generation of ultrastable microwaves via optical frequency division," Nat. Photonics **5**, 425–429 (2011).
22. J. Millo, R. Boudot, M. Lours, P. Y. Bourgeois, A. N. Luiten, Y. L. Coq, Y. Kersalé, and G. Santarelli, "Ultra-low-noise microwave extraction from fiber-based optical frequency comb," Opt. Lett. **34**, 3707–3709 (2009).
23. F. R. Giorgetta, W. C. Swann, L. C. Sinclair, E. Baumann, I. Coddington, and N. R. Newbury, "Optical two-way time and frequency transfer over free space," Nat. Photonics **7**, 434–438 (2013).
24. J. Ye, J. L. Peng, R. J. Jones, K. W. Holman, J. L. Hall, D. J. Jones, S. A. Diddams, J. Kitching, S. Bize, J. C. Bergquist, L. W. Hollberg, L. Robertsson, and L. S. Ma, "Delivery of high-stability optical and microwave frequency standards over an optical fiber network," J. Opt. Soc. Am. B **20**, 1459–1467 (2003).
25. K. Jung, J. Shin, J. Kang, S. Hunziker, C. K. Min, and J. Kim, "Frequency comb-based microwave transfer over fiber with 7×10^{-19} instability using fiber-loop optical-microwave phase detectors," Opt. Lett. **39**, 1577–1580 (2014).
26. S. M. Foreman, K. W. Holman, D. D. Hudson, D. J. Jones, and J. Ye, "Remote transfer of ultrastable frequency references via fiber networks," Rev. Sci. Instrum. **78**, 021101 (2007).
27. S. Droste, F. Ozimek, T. Udem, K. Predehl, T. W. Hansch, H. Schnatz, G. Grosche, and R. Holzwarth, "Optical-frequency transfer over a single-span 1840 km fiber link," Phys. Rev. Lett. **111**, 110801 (2013).
28. I. Coddington, W. C. Swann, L. Lorini, J. C. Bergquist, Y. Le Coq, C. W. Oates, Q. Quraishi, K. S. Feder, J. W. Nicholson, P. S. Westbrook, S. A. Diddams, and N. R. Newbury, "Coherent optical link over hundreds of metres and hundreds of terahertz with subfemtosecond timing jitter," Nat. Photonics **1**, 283–287 (2007).

29. J. Kim, J. A. Cox, J. Chen, and F. X. Kartner, "Drift-free femtosecond timing synchronization of remote optical and microwave sources," Nat. Photonics **2**, 733–736 (2008).

30. J. F. Cliche, B. Shillue, C. Latrasse, M. Tetu, and L. D'Addario, "A high coherence, high stability laser for the photonic local oscillator distribution of the Atacama Large Millimeter Array," in *Ground-Based Telescopes, Parts 1 and 2*, J. M. Oschmann, ed. (2004), pp. 1115–1126.

31. N. R. Nand, J. G. Hartnett, E. N. Ivanov, and G. Santarelli, "Ultra-stable very-low phase-noise signal source for very long baseline interferometry using a cryocooled sapphire oscillator," IEEE Trans. Microw. Theory Tech. **59**, 2978–2986 (2011).

32. G. D. Cole, W. Zhang, M. J. Martin, J. Ye, and M. Aspelmeyer, "Tenfold reduction of Brownian noise in high-reflectivity optical coatings," Nat. Photonics **7**, 644–650 (2013).

33. T. Kessler, C. Hagemann, C. Grebing, T. Legero, U. Sterr, F. Riehle, M. J. Martin, L. Chen, and J. Ye, "A sub-40-mHz-linewidth laser based on a silicon single-crystal optical cavity," Nat. Photonics **6**, 687–692 (2012).

34. D. Matei, T. Legero, S. Häfner, C. Grebing, R. Weyrich, W. Zhang, L. Sonderhouse, J. Robinson, J. Ye, F. Riehle, and U. Sterr, "1.5 µm lasers with sub 10 mHz linewidth," arXiv:1702.04669 (2017).

35. L. C. Sinclair, I. Coddington, W. C. Swann, G. B. Rieker, A. Hati, K. Iwakuni, and N. R. Newbury, "Operation of an optically coherent frequency comb outside the metrology lab," Opt. Express **22**, 6996–7006 (2014).

36. N. Kuse, J. Jiang, C.-C. Lee, T. Schibli, and M. Fermann, "All polarization-maintaining Er fiber-based optical frequency combs with nonlinear amplifying loop mirror," Opt. Express **24**, 3095–3102 (2016).

37. M. Lezius, T. Wilken, C. Deutsch, M. Giunta, O. Mandel, A. Thaller, V. Schkolnik, M. Schiemangk, A. Dinkelaker, and A. Kohfeldt, "Space-borne frequency comb metrology," Optica **3**, 1381–1387 (2016).

38. J. E. Stalnaker, S. A. Diddams, T. M. Fortier, K. Kim, L. Hollberg, J. C. Bergquist, W. M. Itano, M. J. Delany, L. Lorini, W. H. Oskay, T. P. Heavner, S. R. Jefferts, F. Levi, T. E. Parker, and J. Shirley, "Optical-to-microwave frequency comparison with fractional uncertainty of 10^{-15}," Appl. Phys. B **89**, 167–176 (2007).

39. L. S. Ma, Z. Y. Bi, A. Bartels, L. Robertsson, M. Zucco, R. S. Windeler, G. Wilpers, C. Oates, L. Hollberg, and S. A. Diddams, "Optical frequency synthesis and comparison with uncertainty at the 10^{-19} level," Science **303**, 1843–1845 (2004).

40. Y. Yao, Y. Jiang, H. Yu, Z. Bi, and L. Ma, "Optical frequency divider with division uncertainty at the 10^{-21} level," Natl. Sci. Rev. **3**, 463–469 (2016).

41. C. Hagemann, C. Grebing, T. Kessler, S. Falke, N. Lemke, C. Lisdat, H. Schnatz, F. Riehle, and U. Sterr, "Providing short-term stability of a 1.5-laser to optical clocks," IEEE Trans. Instrum. Meas. **62**, 1556–1562 (2013).

42. H. Inaba, Y. Daimon, F. L. Hong, A. Onae, K. Minoshima, T. R. Schibli, H. Matsumoto, M. Hirano, T. Okuno, M. Onishi, and M. Nakazawa, "Long-term measurement of optical frequencies using a simple, robust and low-noise fiber based frequency comb," Opt. Express **14**, 5223–5231 (2006).

43. Y. Nakajima, H. Inaba, K. Hosaka, K. Minoshima, A. Onae, M. Yasuda, T. Kohno, S. Kawato, T. Kobayashi, and T. Katsuyama, "A multi-branch, fiber-based frequency comb with millihertz-level relative linewidths using an intra-cavity electro-optic modulator," Opt. Express **18**, 1667–1676 (2010).

44. I. Ushijima, M. Takamoto, M. Das, T. Ohkubo, and H. Katori, "Cryogenic optical lattice clocks," Nat. Photonics **9**, 185–189 (2015).

45. N. Ohmae, N. Kuse, M. Fermann, and H. Katori, "All-polarization-maintaining, single-port Er:fiber comb for high-stability comparison of optical lattice clocks," Appl. Phys. Express **10**, 062503 (2017).

46. D. Nicolodi, B. Argence, W. Zhang, R. Le Targat, G. Santarelli, and Y. Le Coq, "Spectral purity transfer between optical wavelengths at the 10^{-18} level," Nat. Photonics **8**, 219–223 (2014).

47. L. E. Nelson, D. J. Jones, K. Tamura, H. A. Haus, and E. P. Ippen, "Ultrashort-pulse fiber ring lasers," Appl. Phys. B **65**, 277–294 (1997).

48. T. Okuno, M. Onishi, T. Kashiwada, S. Ishikawa, and M. Nishimura, "Silica-based functional fibers with enhanced nonlinearity and their applications," IEEE J. Sel. Top. Quantum Electron. **5**, 1385–1391 (1999).

49. M. J. Martin, S. M. Foreman, T. Schibli, and J. Ye, "Testing ultrafast mode-locking at microhertz relative optical linewidth," Opt. Express **17**, 558–568 (2009).

50. J. Stenger, H. Schnatz, C. Tamm, and H. R. Telle, "Ultraprecise measurement of optical frequency ratios," Phys. Rev. Lett. **88**, 073601 (2002).

51. D. B. Sullivan, D. W. Allan, D. A. Howe, and F. L. Walls, *Characterization of Clocks and Oscillators* (National Institute of Standards and Technology Technical Note, 1990).

52. D. Yeaton-Massey and R. X. Adhikari, "A new bound on excess frequency noise in second harmonic generation in PPKTP at the 10^{-19} level," Opt. Express **20**, 21019–21024 (2012).

53. M. Zimmermann, C. Gohle, R. Holzwarth, T. Udem, and T. W. Hänsch, "Optical clockwork with an offset-free difference-frequency comb: accuracy of sum-and difference-frequency generation," Opt. Lett. **29**, 310–312 (2004).

54. S. T. Dawkins, J. J. McFerran, and A. N. Luiten, "Considerations on the measurement of the stability of oscillators with frequency counters," IEEE Trans. Ultrason. Ferroelectr. Freq. Control **54**, 918–925 (2007).

55. T. M. Fortier, J. Ye, S. T. Cundiff, and R. S. Windeler, "Nonlinear phase noise generated in air–silica microstructure fiber and its effect on carrier–envelope phase," Opt. Lett. **27**, 445–447 (2002).

56. L. Johnson, P. Gill, and H. Margolis, "Evaluating the performance of the NPL femtosecond frequency combs: agreement at the 10^{-21} level," Metrologia **52**, 62–71 (2015).

57. T. Fortier, A. Rolland, F. Quinlan, F. Baynes, A. Metcalf, A. Hati, A. Ludlow, N. Hinkley, M. Shimizu, and T. Ishibashi, "Optically referenced broadband electronic synthesizer with 15 digits of resolution," Laser Photon. Rev. **10**, 780–790 (2016).

58. S. A. Diddams, T. Udem, J. C. Bergquist, E. A. Curtis, R. E. Drullinger, L. Hollberg, W. M. Itano, W. D. Lee, C. W. Oates, K. R. Vogel, and D. J. Wineland, "An optical clock based on a single trapped Hg ion," Science **293**, 825–828 (2001).

59. L. S. Ma, P. Jungner, J. Ye, and J. L. Hall, "Delivering the same optical frequency at two places: accurate cancellation of phase noise introduced by an optical fiber or other time-varying path," Opt. Lett. **19**, 1777–1779 (1994).